*Acta Oceanol. Sin.*, 2024, Vol. 43, No. 11, P. 118–130
https://doi.org/10.1007/s13131-024-2437-1
http://www.aosocean.com
E-mail: ocean2@hyxb.org.cn

# Analysis of coastline changes and influencing factors for the Macao Special Administrative Region based on Neural Network Algorithms

Xiaofang Jiang[1, 2, 3, 4*], Feijian Yin[5]

[1] School of Geographical Sciences, Qinghai Normal University, Xining 810016, China

[2] Key Laboratory of Tibetan Plateau Land Surface Processes and Ecological Conservation (Ministry of Education), Qinghai Normal University, Xining 810016, China

[3] Qinghai Provincial Key Laboratory of Physical Geography and Environmental Process/College of Geographical Science, Qinghai Normal University, Xining 810016, China

[4] Academy of Plateau Science and Sustainability, People's Government of Qinghai Province and Beijing Normal University, Xining 810016, China

[5] Third Institute of Oceanography, Ministry of Natural Resources, Xiamen 361005, China

Received 25 April 2024; accepted 24 June 2024



**Abstract**

The Macao Special Administrative Region is located in the southeastern coastal area of China. The region of Macao was narrow in the history, so land reclamation has become a main means of expanding its geographical scope. Exploring the significance of land reclamation for the planning and urban construction of the Macao region provides valuable references. (1) The Google Earth Engine (GEE) cloud processing platform is used in this study to calculate the modified normalized difference water index (MNDWI) based on Landsat data from 1986 to 2021; (2) the Jenks natural index classification method is used to extract the water body range, and the water body boundary as well as area at different periods is calculated combined with the neural network classification method in the environment for visualizing images (ENVI) software; (3) this study then combines the patch-generating land use simulation (PLUS) model to predict the future trend of shoreline changes in the study area in 2036. The result indicates that the MNDWI and neural net classification method lead to a high classification accuracy with both the overall accuracy (OA) and Kappa coefficient being higher than 87%. Land reclamation activities in Macao were gradually intense from 1986 to 2021, with social and economic conditions such as transportation being main influencing factors, which provides valuable references and inspiration for the regional planning of the Macao Special Administrative Region.

**Key words:** Macao Special Administrative Region, Google Earth Engine, reclamation of land from the sea, water body index, water boundary

**Citation:** Jiang Xiaofang, Yin Feijian. 2024. Analysis of coastline changes and influencing factors for the Macao Special Administrative Region based on Neural Network Algorithms. Acta Oceanologica Sinica, 43(11): 118–130, doi: 10.1007/s13131-024-2437-1

## 1 Introduction

Reclaiming land from the sea is an inevitable product of urbanization in coastal areas around the world. The rapid development of industrialization has led to a series of urban problems, such as population explosion, traffic congestion, housing shortage and environmental pollution. Reclaiming land from the sea is beneficial for avoiding and solving these urban problems. Macao is located in the southeastern coastal area of China as an important part of the Guangdong-Hong Kong-Macao Greater Bay Area. Studying changes in the coastline of the Macao Special Administrative Region is beneficial for its socio-economic development.

Remote sensing technology is an important means of assessing changes in the ecological environment and economic-social development of coastal areas (Xie et al., 2022). At present, many studies have been focused on shoreline changes and marine ecological environment in the Zhujiang River Estuary area. Liu et al. (2017) processed remote sensing data of eight periods in the Zhujiang River Estuary area, including six cities of Guangdong Province from 1973 to 2015 using the object-oriented method, obtaining coastline changes in the study area while carrying out a driving force analysis. Wang et al. (2016) utilized the object-oriented and supervised classification methods to monitor coastline changes in the Zhujiang River Estuary, including five cities of Guangdong Province from 1960 to 2012. Yang et al. (2021) used six remote sensing images from 1986 to 2018 to study spatiotemporal changes in the shoreline changes of the Guangdong-Hong Kong-Macao region. Existing research is mainly focused on the coastal changes in local cities of Guangdong-Hong Kong-Macao Greater Bay Area during a few periods, without conducting research on their long-term continuous changes. Macao is located in the Zhujiang River Estuary region, with a small area of available and intensive land reclamation activities. There is currently a lack of research on annual shoreline changes in the Macao region. Monitoring and analysis of the annual shoreline changes in Macao Special Administrative Region can obtain more detailed trends of shoreline changes. Combining Google Earth Engine with neural network algorithm can improve the accuracy of extraction. Traditional methods for extracting water bodies from

*Corresponding author, E-mail: 1695090635@qq.com

images mainly include threshold method, spectral index method, object-oriented method based on texture and spectral features, as well as machine learning method. With the rapid development and improvement of machine learning method, neural networks are widely used in fields such as water detection, land use classification, change detection, semantic segmentation and quantitative remote sensing (Feng et al., 2022b). Some machine learning methods like convolutional neural networks (CNNs), generative adversarial networks (GANs) and fully-convolutional neural networks (FCNs) improve the accuracy of water extraction by increasing the depth of hidden layers. The process of machine learning for water body extraction first involves inputting remote sensing images and labeled samples; then extracting water features such as textures and spectra, and methods such as upsampling convolution, deconvolution and multi-scale segmentation are used to segment water areas; finally, the results are post-processed by combining morphologies, conditional random fields and face objects (Duan and Hu, 2020; Feng et al., 2019; Hertel et al., 2023; Lu et al., 2022; Weng et al., 2020). Bendixen et al. (2017) conducted a comprehensive investigation of the Arctic Delta by plotting the coastal morphology dynamics of 121 Greenland deltas from 1940s to 2010s, finding that with climate warming, the increase in freshwater runoff and sediment flux led to a gradual expansion of the delta area. The negative AMO is associated with a continued acceleration of sea-level rise along the northeast coast of the United States (McCarthy et al., 2015). Changes in the coastal zones are an important reflection of the development of social, economic, and natural conditions, which mainly manifest shorter shorelines and smaller water areas, having a significant impact on water dynamic conditions, waves and currents. The main focus of research is on coastal zone changes, beach restoration, the monitoring of marine ecological environment as well as the monitoring and management of coastal vegetation (Dai et al., 2019; Islam et al., 2019). Therefore, it is imperative to monitor and restore the ecological environment of coastal zones over a long period of time.

Land classification and water extraction technologies have gone through a development process from mathematical statistics, optical wave analysis transformation and traditional image processing methods to machine learning algorithm (Ahmad et al., 2020; Yang et al., 2018; Yao et al., 2019). The emergence of machine learning has laid a solid foundation for the application of remote sensing technology. Using machine learning, features related to classification tasks can be adaptively extracted, but due to the complex network structure of deep learning, a large number of training samples are required to improve the accuracy of prediction and classification (Feng et al., 2022a). The use of neural network technology in the field of geospatial remote sensing is becoming increasingly widespread, such as back propagation neural network (BPNN), deep neural network (DNN) and recurrent neural network (RNN) (Pham et al., 2017; Wang et al., 2018; Wei et al., 2022; Zhang et al., 2022a). The U-net algorithm has an extremely high efficiency in image processing. The AlexNet algorithm outperformed other image segmentation methods in terms of classification accuracy; in 2015, fully-connected neural network (FCN) emerged, achieving an end-to-end pixel level classification (Hinton and Salakhutdinov, 2006; Chen et al., 2018). The main characteristics of convolution operations are local connections and weight sharing, while pooling operations can satisfy evaluation invariance. The FCN adopts techniques such as skip layer structure, residual and dilated convolution, etc., which can achieve the task of target multi-scale information, reconstruct original image information and save image spatial information from graph to graph (Zhang et al., 2020).

As an important coastal city in China, Macao is a typical area for land reclamation. So, this study chooses Macao as the research object. The modified normalized difference water index (MNDWI) is an important water index improved from normalized difference water index (NDWI), which is usually used to extract water areas in many studies (Xu, 2005; Karaman, 2021). The patch-generating land use simulation (PLUS) is often effectively utilized to predict land use transition (Li et al., 2022; Zhang et al., 2022b). Layered feed forward neural network classification in the environment for visualizing images (ENVI) is an effective method. Neural network algorithm is a highly-robust and applicable image processing algorithm (Garajeh et al., 2021; Yang et al., 2020), which has a wide range of applications in land use classification and water extraction. Using Google Earth Engine (GEE), MNDWI, PLUS and neural net classification, this study explores shoreline changes in the study area, reveals the development process of land reclamation in the area, and combines natural environmental socio-economic factors such as transportation, terrain, GDP as well as population to explore the future development trend of land reclamation in the area based on the PLUS model, which provides valuable references for the Government's urban development decision-making and planning.

## 2 Study area and study methods

### 2.1 *Introduction of study area*

The Macao Special Administrative Region is located around the South China Sea in the southeastern coastal area of China, with longitude and latitude positioned at 22°11′ N, 113°33′ E (Fig. 1). The climate type of this area is subtropical monsoon humid climate. There are higher temperatures, more precipitation and higher humidity in summer, with a is relatively warm and dry climate in winter. The geographical area of Macao is 32.8 km$^2$, with a relatively low and flat terrain. The economic pillar of Macao is secondary and tertiary industries, which have a high demand for urban geographical scope.

### 2.2 *Study methods*

This study first uses GEE to obtain Landsat remote sensing image data of the study area, then the MNDWI water body index is calculated, and the possible range of water bodies is obtained based on Jenks natural breakpoint method. We establish a region of interest based on the water body range delineated by Jenks, and then use the neural net classification method of ENVI software for water body classification research (Fig. 2).

#### 2.2.1 *Remote sensing image processing based on GEE*

The GEE platform is currently a widely-used remote sensing image processing platform that can efficiently process remote sensing image data, providing remote sensing and ecological environment workers with a large amount of data on free long time series remote sensing images as well as a large number of function algorithms, which can easily implement various algorithms, and is compatible with both JavaScript and Python languages, providing convenience for different researchers to conduct scientific research. This study conducts cloud removal and other preprocessing on Landsat remote sensing image data from 1986 to 2021 using GEE. Finally, we use the mean of annual remote sensing images as the data source in the water extraction research. Due to the large number of Landsat images in the same region each year, representing different time periods, we have taken the mean of remote sensing image data in different time periods throughout the year as a representative of remote sens-

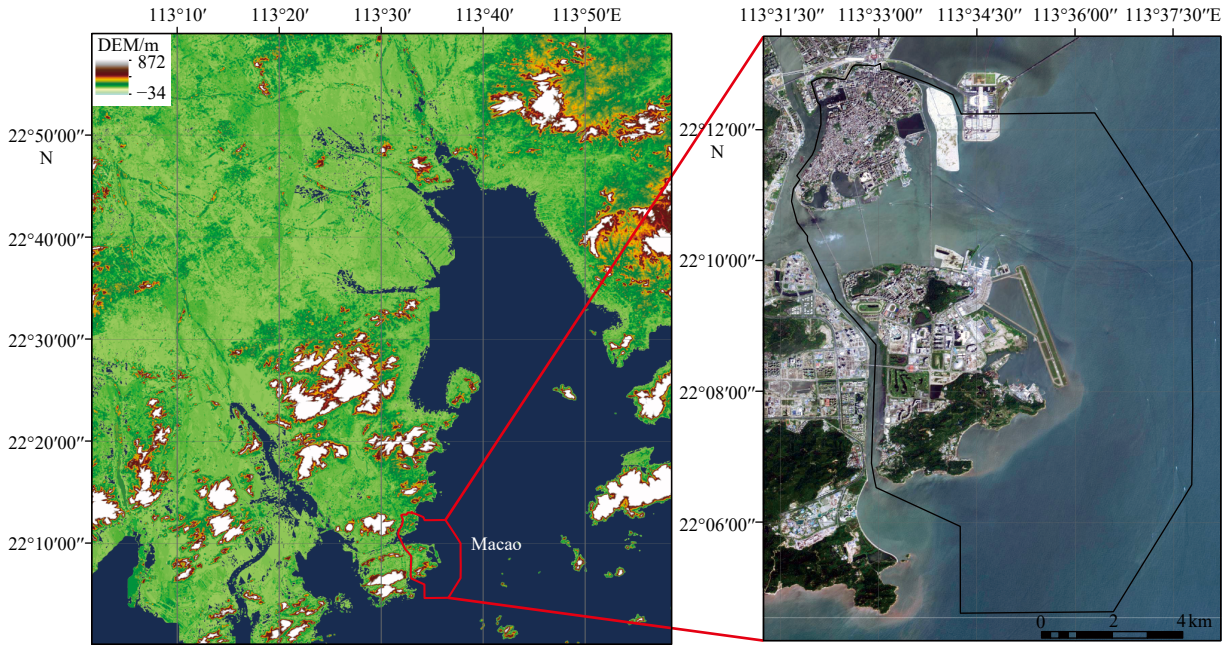


**Fig. 1.** Introduction to the location of the study area with the Digital Elevation Model and the remote sensing data.

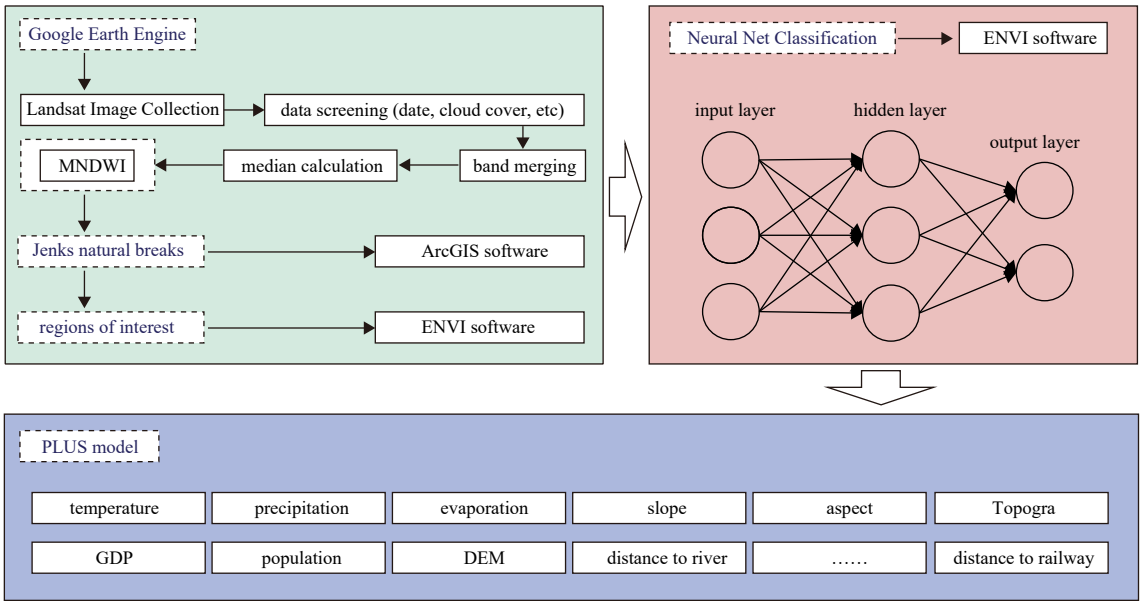


**Fig. 2.** Research technology flow chart.

ing images for that year. However, it was difficult to obtain high-quality remote sensing image data in 2012 because there were many stripes in the image, so this study excludes that year. Common indicators include visually-discernible coastal features used in this study and tidal datum-based coastline features.

2.2.2 *MNDWI water index and Jenks water range extraction*

The MNDWI is based on mid infrared and green bands, derived from NDWI, and has been improved to reduce interferences from high-rise buildings in cities for water area detection. The Jenks natural breakpoint method can be used to effectively classify data and identify differences among different land use patches, whose classification principle is "the minimum intra-class difference and the maximum inter-class difference". The formula for MNDWI is as follows:

$$\mathrm{MNDWI} = (G - \mathrm{SWIR})/(G + \mathrm{SWIR}), \tag{1}$$

where $G$ represents the reflectance of green bands, and SWIR represents the reflectance of shortwave infrared bands.

2.2.3 *Neural net classification and PLUS model*

Neural network algorithms belong to machine learning algorithms. Ordinary neural networks mainly include input layers, hidden layers and output layers, each with several neurons, which can achieve functions such as pattern recognition and intelligent control. The neural net classification algorithm in ENVI is a layered feed forward neural network classification.

The PLUS model is a land use spatial distribution and prediction model developed in recent years, which adopts the random forest classification method while combining natural or socio-economic factors to analyze the driving factors of land use changes, and then predicts the future distribution patterns of land use patches. This study uses the PLUS model to predict the future distribution of water bodies in the region. Because coastline changes in Macao are mainly due to its tight land area caused by socio-economic development, the government adopts the method of land reclamation to expand urban land area. Therefore, this study chooses these influencing factors for predictive research. The information of influencing factors is shown in the Table 1.

2.2.4 *Evaluation of water extraction accuracy*

This study uses overall accuracy (OA) and Kappa accuracy evaluation methods to evaluate the accuracy of water extraction. The formulas for OA and Kappa are as follows:

$$\mathrm{OA} = (\mathrm{TP} + \mathrm{TN})/(\mathrm{TP} + \mathrm{TN} + \mathrm{FP} + \mathrm{FN}), \tag{2}$$

$$\mathrm{Kappa} = (P_0 - P_\mathrm{E})/(1 - P_\mathrm{E}), \tag{3}$$

where, TP represents the true number of cases, TN represents the true negative number of cases, FP represents the false positive number of cases, and FN represents the false negative number of cases. $P_0$ is the sum of the number of correctly-classified samples for each class divided by the total number of samples, which is the overall classification accuracy. $P_\mathrm{E}$ is the sum of the products of the actual and predicted number of samples, divided by the square of the total number of samples.

## 3 Results

### 3.1 *Verification results of accuracy of water extraction range*

This study selects 100 sample points in both water and non-water bodies respectively as validation data sources to validate the water extraction areas from 1986 to 2021 (Figs 3 and 4). The results show that the water extraction accuracy of both OA and Kappa coefficient are higher than 87% year by year during this period (Fig. 5).

### 3.2 *The changes in the coastline of Macao*

Macao is mainly divided into Macao Peninsula, Taipa Island and Coloane Island. From 1986 to 2021, the land area of the study area showed a fluctuating upward trend, while the water area gradually decreased (Figs 6 and 7). From 1986 to 1991, areas with significant changes in coastline were mainly located on Macao Peninsula. In 1986, the Bei'an Industrial Zone in the northeast of Taipa, the Ocean Garden residential area in the west, the Liansheng Industrial Village in the northwest of Coloane, as well as the cement plant and oil depot in the northeast were successively reclaimed from the sea. From 1991 to 1996, coastline changes in Taipa Island and Coloane Island were quite typical. From 1987 to 1996, Macao Peninsula carried out another large-scale reclamation project in history, mainly including the Black Sand Ring Reclamation Project, the Outer Harbor Reclamation Project and the South Bay Lake Reclamation Project, as well as some small projects in the northwest and south ends of the peninsula; Taipa has carried out larger-scale reclamation projects, including the expansion of international airports and racetracks; Coloane has also completed land reclamation for Jiu'ao Port and power plants, as well as for hotels and residential areas on both sides of the Heisha Bay. From 1996 to 2001, regional coastline changes between Taipa Island and Coloane Island were quite typical. The Taipa City Reclamation Project was launched in 1997 and completed in 2006, during which, some reclamation projects were carried out on Macao Peninsula, such as the Qingzhou Cross Border Industrial Zone and the Vicinity of Chopsticks Base. The most famous offshore reclamation project was the Cotai City Reclamation Project on both sides of the Cotai Expressway, which began in the late 1990s. In the following decade, the area between Taipa Island and Coloane Island remained in a state of land reclamation, which lasted until 2011. After 2006, Macao successively improved the Cotai Reclamation Project in the eastern part of the airport (which has been completed) and launched a new "Macao New City" Reclamation Plan. After 2011, land reclamation in the Macao region mainly occurred on Macao Peninsula.

### 3.3 *Analysis of main factors of land reclamation in Macao*

This study uses factors such as population, GDP, transportation and building density to analyze the main influencing factors of land reclamation (Fig. 8). Perhaps because Macao's GDP has always been at a stable growth level, its impact on Macao's land and water changes is smaller than other factors. The main influencing factors of shoreline changes from 1986 to 1996 were transportation and terrain, while those of shoreline changes from 1996 to 2006 were also transportation and rainfall. From 2006 to 2016, the proportion of natural factors in shoreline changes was relatively high. During the period from 2016 to 2021, transportation

**Table 1.** Data introduction of different influencing factors

| Influence factor | Spatial resolution | Reference |
|---|---|---|
| Precipitation | 1 km | https://www.resdc.cn/Default.aspx |
| Temperature | 1 km | https://www.resdc.cn/Default.aspx |
| Slope | 30 m | https://www.gscloud.cn/ |
| Elevation | 30 m | https://www.gscloud.cn/ |
| Aspect | 30 m | https://www.gscloud.cn/ |
| GDP | 1 km | https://www.resdc.cn/Default.aspx |
| Population | 1 km | https://www.resdc.cn/Default.aspx |
| Distance from road | 30 m | https://www.openstreetmap.org/ |
| Distance from river | 30 m | https://www.openstreetmap.org/ |
| Distance from railways | 30 m | https://www.openstreetmap.org/ |
| Geomorphology | 30 m | https://www.resdc.cn/Default.aspx |
| Evaporation | 30 m | https://www.resdc.cn/Default.aspx |

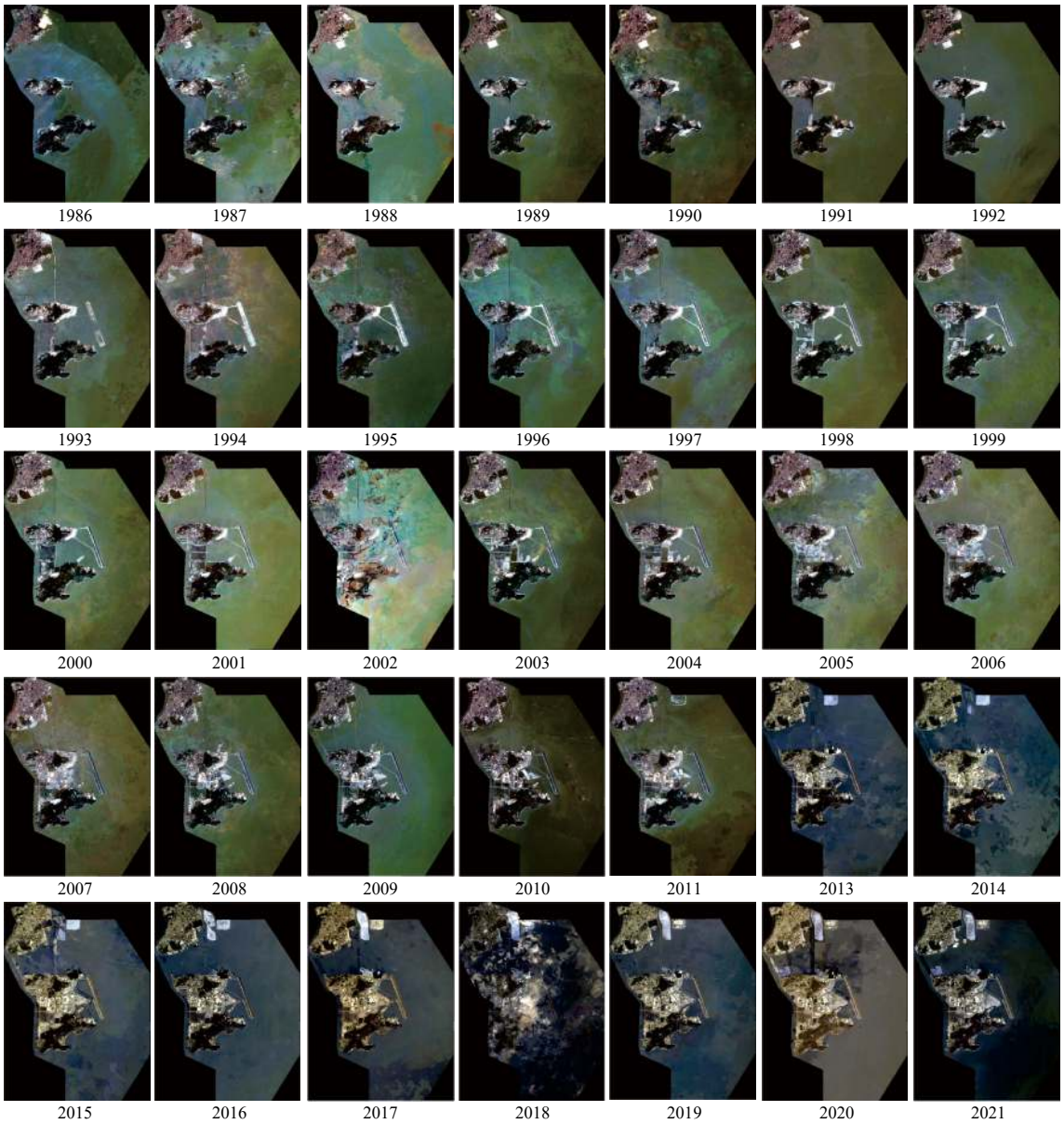


**Fig. 3.** Original remote sensing image data of the research area.

also had a significant impact on shoreline changes. Therefore, transportation, among natural factors, is the main influencing factor of shoreline changes in the study area. Because Macao is mainly dominated by secondary and tertiary industries, especially gambling tourism industry in the tertiary sector, socio-economic factors play a dominant role in land reclamation and coastline changes. Meanwhile, all the roads built during these reclamation projects are used for secondary and tertiary industry lands, which are economic, such as the Black Sand Ring Outer Port Nansha Lake Reclamation Project on Macao Peninsula and the Cotai Reclamation Project on Taipa Island as well as Coloane Island. The latter is connected by the Cotai Expressway, so transportation factors play a crucial role in the transformation of the Macao coastline.

### 3.4 *The development process of future land reclamation in Macao*

We use natural and socio-economic driving force data and water classification data from 2006 to 2021 as data sources, and predict the land reclamation situation of Macao in 2036 based on the PLUS model (Fig. 9). The results indicate that future land reclamation will mainly occur in the surrounding areas of existing land reclamation, namely the eastern region of Macao Peninsula and the northeast region of Taipa and Coloane. However, the PLUS model predicts that there may be land protrusions in the sea area in the future, which may be caused by natural factors. Natural conditions of the sea area are relatively good, and the research area has also experienced a land reclamation far from lands.

## 4 Discussion

### 4.1 *Comparison of different water extraction methods*

Neural networks based on machine learning algorithms are an important and effective method for land use patch classification, which can intelligently serve shoreline monitoring. We use a layered feed-forward neural network classification algorithm for water range extraction and achieved a high validation accuracy, indicating that neural network algorithms can be effectively ap-


**Fig. 4.** Extraction of water body range of the study area.

plied to water range extraction. This method is more effective than traditional band ratio methods, threshold methods and image edge detection methods (Feyisa et al., 2014; Wang et al., 2010; Liu et al., 2017; Sunder et al., 2017). In addition, our result is similar to that of other studies using machine learning methods. Li et al. (2019) proposed a SAR image change detection algorithm based on CNNs, through which false labels are first generated through unsupervised spatial fuzzy clustering, then these samples are filtered to train the neural networks, and results are obtained through the trained CNN. Gao et al. (2019) proposed a CWNN algorithm and the result demonstrated the effectiveness and robustness of the method. Neural networks have advantages such as processing large-scale and temporal data, multi-level feature extraction methods, local connections and weight sharing, so they still have good performance in water extraction. Image classification technology has also been widely applied in shoreline and water range extraction, evolving from visual interpretation to supervised and unsupervised classification, as well as to current machine learning technologies, where classification methods have evolved from pixel-based to object-based (Chen et al., 2022; Gong et al., 2012; Hochberg, 2003; Hu and Ban, 2014; Li et al., 2022; Mcfeeters, 1996; Purkis et al., 2002; Yang et al., 2018). AlexNet, SPP net, NIN, CaffeNet, ZF net and other neural network algorithms have emerged and been widely utilized (Qiu et al., 2020; Tseng and Sun, 2022; Wei et al., 2023; Zhang et al., 2016; Zhao and Du, 2016). Wang et al. (2017) proposed a variance method for extracting discriminative image features from the same same-level information contained in CNNs. Hinton and Salakhutdinov (2006) studied a deep auto-encoder network learning method that could effectively initialize weights, which is more efficient than principal component analyses. Chen et al. (2018) integrated the final DCNN layer with the CRF and got improved localization performance. Ge et al. (2022) proved that the improved U-net algorithm performed better than traditional methods, while other studies got the similar result (Chen et al., 2020; Duan and Hu, 2020; Lu et al., 2022; Wang and Wang,

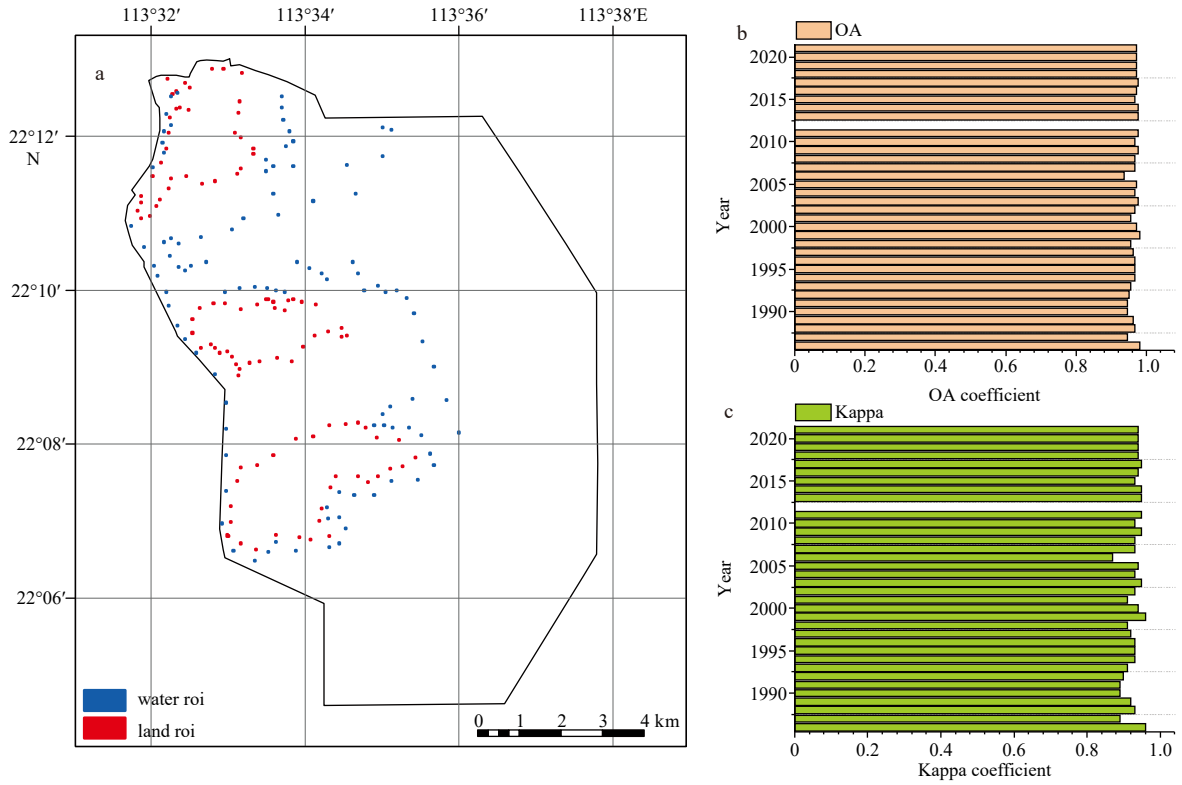


**Fig. 5.** Water roi and land roi (a), OA (b), and Kappa (c) coefficient for the extraction accuracy of water body range in the study area.

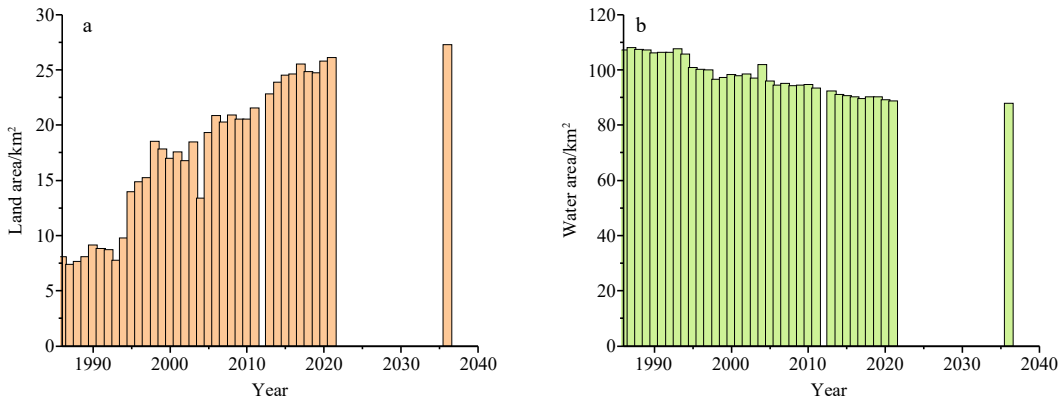


**Fig. 6.** Land and water area values at different periods.

2019; Weng et al., 2020; Zhang et al., 2017a, 2018, 2023). Therefore, many studies used CNNs for water area extraction, and the accuracy of the algorithms was relatively high (Gao et al., 2019; Li et al., 2018; Nemni et al., 2020; Tseng and Sun, 2022). In the future, neural networks will gradually be improved to enhance their applications in the field of image analysis, and their applications in the water area extraction field will be more extensive.

### 4.2 *Application of different data sources in water extraction*

In this study, we use Landsat remote sensing image data for water range extraction. The accuracy verification results of water body extraction showed a high accuracy, indicating that Landsat has a relatively high spatial resolution and can be applied to water body range extraction. There are many studies using Landsat remote sensing data in the water research field (Jiang et al., 2018; Rokni et al., 2014; Wang et al., 2018; Zhang et al., 2017b). In addition, other remote sensing images with a high spatial resolution or other advantages are used in the field of water extraction. Adrian et al. (2021) used Sentinel-1 radar data and Sentinel-2 optical data for fusion, and then conducted research to improve classification accuracy. Therefore, we can try to do this in the future when there is no need to make long-time-series analyses. What's more, remote sensing image data is susceptible to factors such as instrument noises, atmospheric conditions and surface conditions. The impact of microwave radar data is mainly manifested in structural sensitivity, imaging distortion, speckle noises and imaging system interferences. One major flaw is speckle noises, which are caused by the interferences of return waves at the radar aperture. Many studies use median filtering methods to smooth remote sensing images (Li et al., 2019). Optical remote sensing images are susceptible to interferences from clouds and atmospheric moisture content, especially in tropical and subtropical regions. Synthetic aperture radar images can effectively

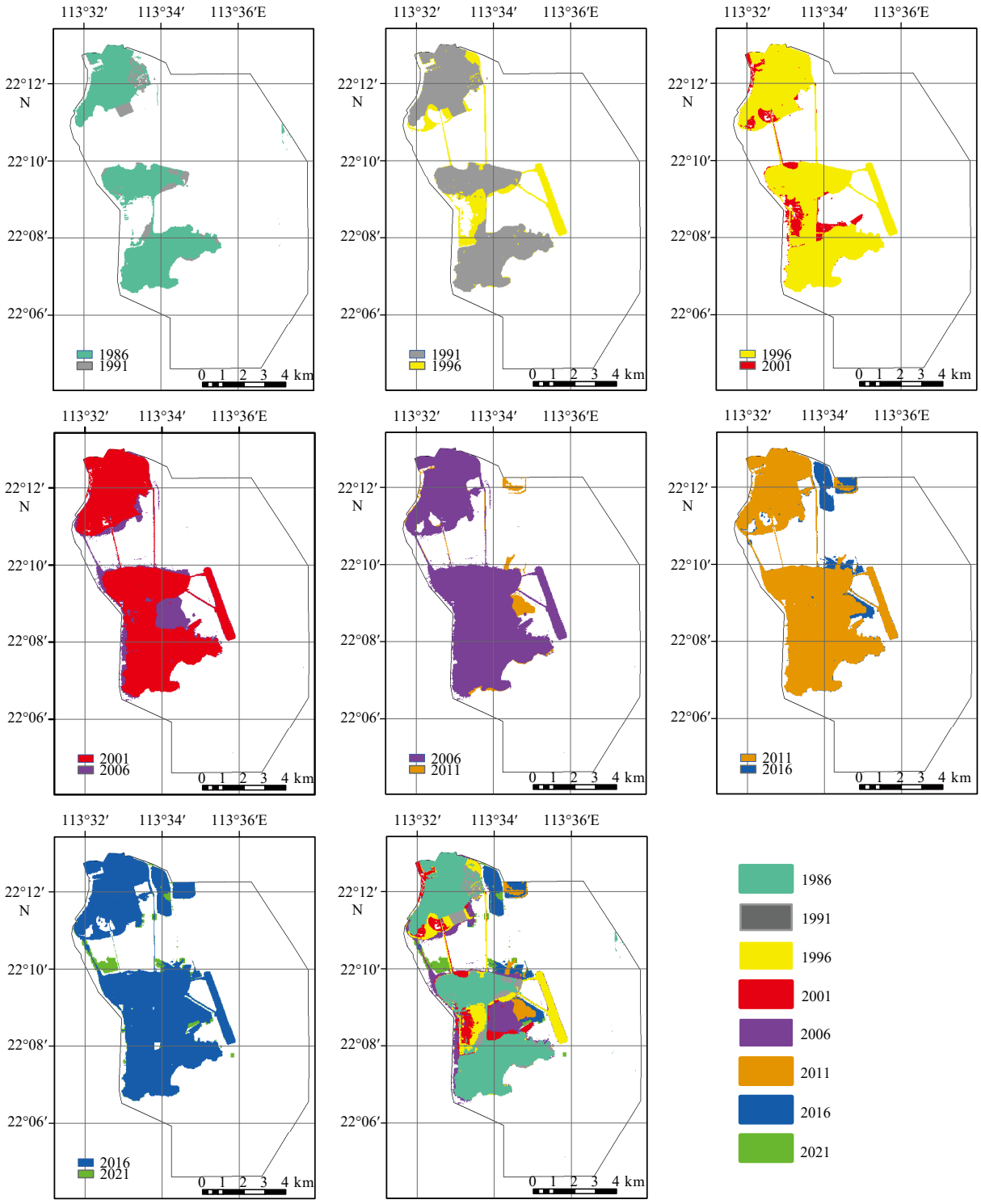


**Fig. 7.** Changes in water body area during different time periods.

avoid such drawbacks, but are susceptible to interferences from terrain and vegetation. Many methods are used to compensate for shortcomings in remote sensing data quality. Li et al. (2020) proposed an object-based fully-convolutional network to overcome interferences from different data sources. Image filtering is an important means of eliminating background noises. Currently, existing filtering methods include mean filtering, median filtering, Gaussian filtering and wavelet filtering (Geusebroek et al., 2003; Saxena and Rathore, 2013). In addition, many studies have fused remote sensing image data from different sensors to carry out coastline change detection, environmental monitoring, forest resource monitoring, leaf area index, land use mapping and other fields (Houborg and McCabe, 2018; Lunetta et al., 2006; Seo et al., 2018; Yousif and Ban, 2014). Rule-based water area classification algorithms fuse optical and radar images to obtain the best results for water masks (Ahmad et al., 2020). With the improvement of scientific and technological level, remote sensing images have been significantly improved in terms of tempor-

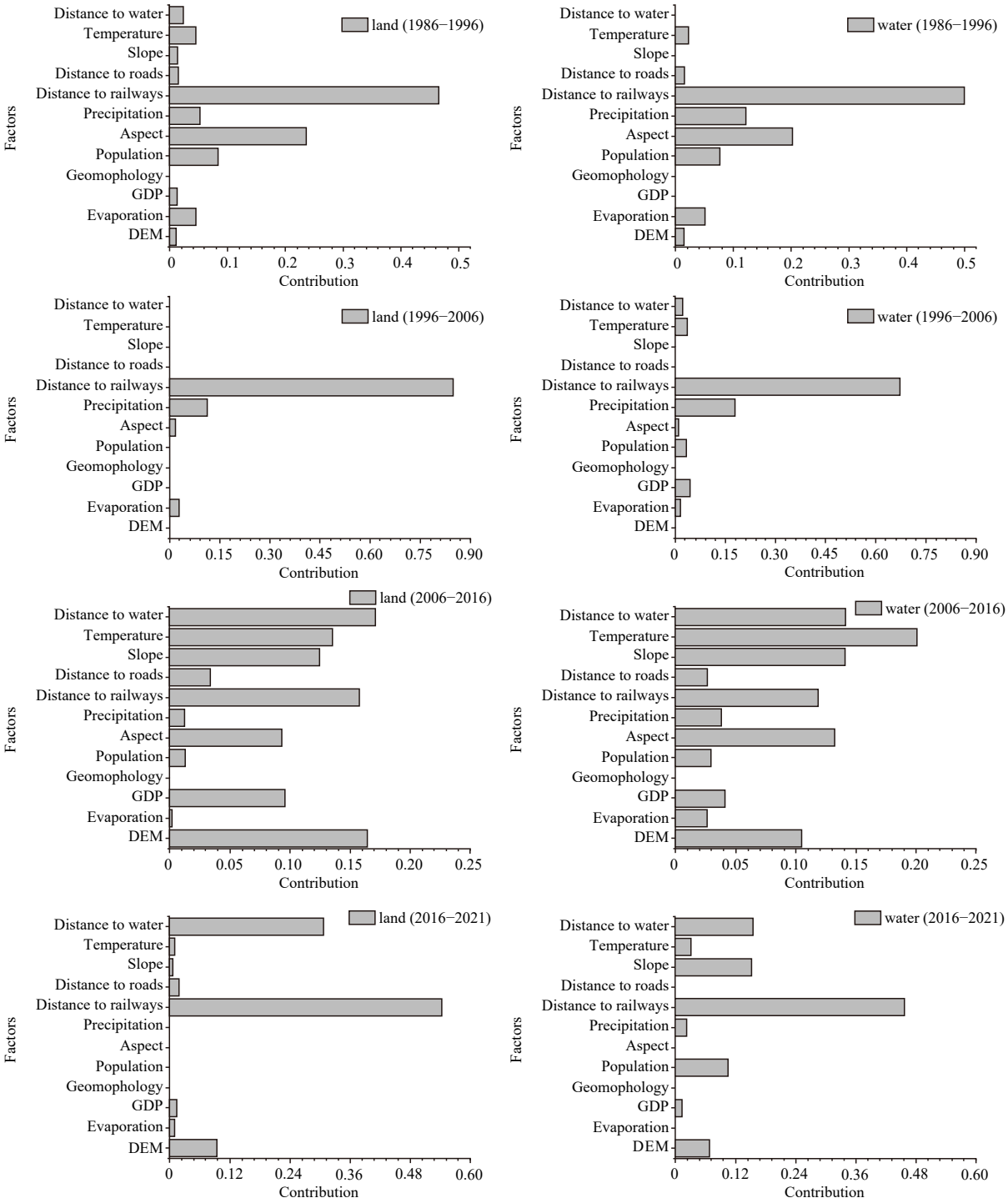


**Fig. 8.** The contribution of multiple factors to shoreline changes in different periods.

al resolution, spatial resolution and spectral resolution. Especially, spatial resolution has developed, and the improvement of spectral resolution has led to the development of remote sensing images from multispectral to hyperspectral level (Andréfouët et al., 2001a, 2001b, 2003; Mumby and Edwards, 2002). Wieland et al. (2023) found that high-resolution satellites (IKONOS, GeoEye-1, WorldView-2, WorldView-3, and four different airborne camera systems) and aerial images could improve model performance. Feng et al. (2019) utilized high-spatial-resolution Gaofen-2 and WorldView-2 remote sensing images to classify images into water and non-water areas. Zhang et al. (2021) demonstrated that Gaofen-3 SAR images could be used to validate the neural network method, while other studies got similar results (Hertel et al., 2023; Nemni et al., 2020; Ni et al., 2021; Xue et al., 2021). With the deepening of research, when extracting water body information in a short period of time, we can make improvements in remote sensing data sources and research methods, and combine the above methods to further improve the accuracy of water body information extraction.

## 5 Conclusions

Due to the narrow geographical scope of Macao, land reclam-

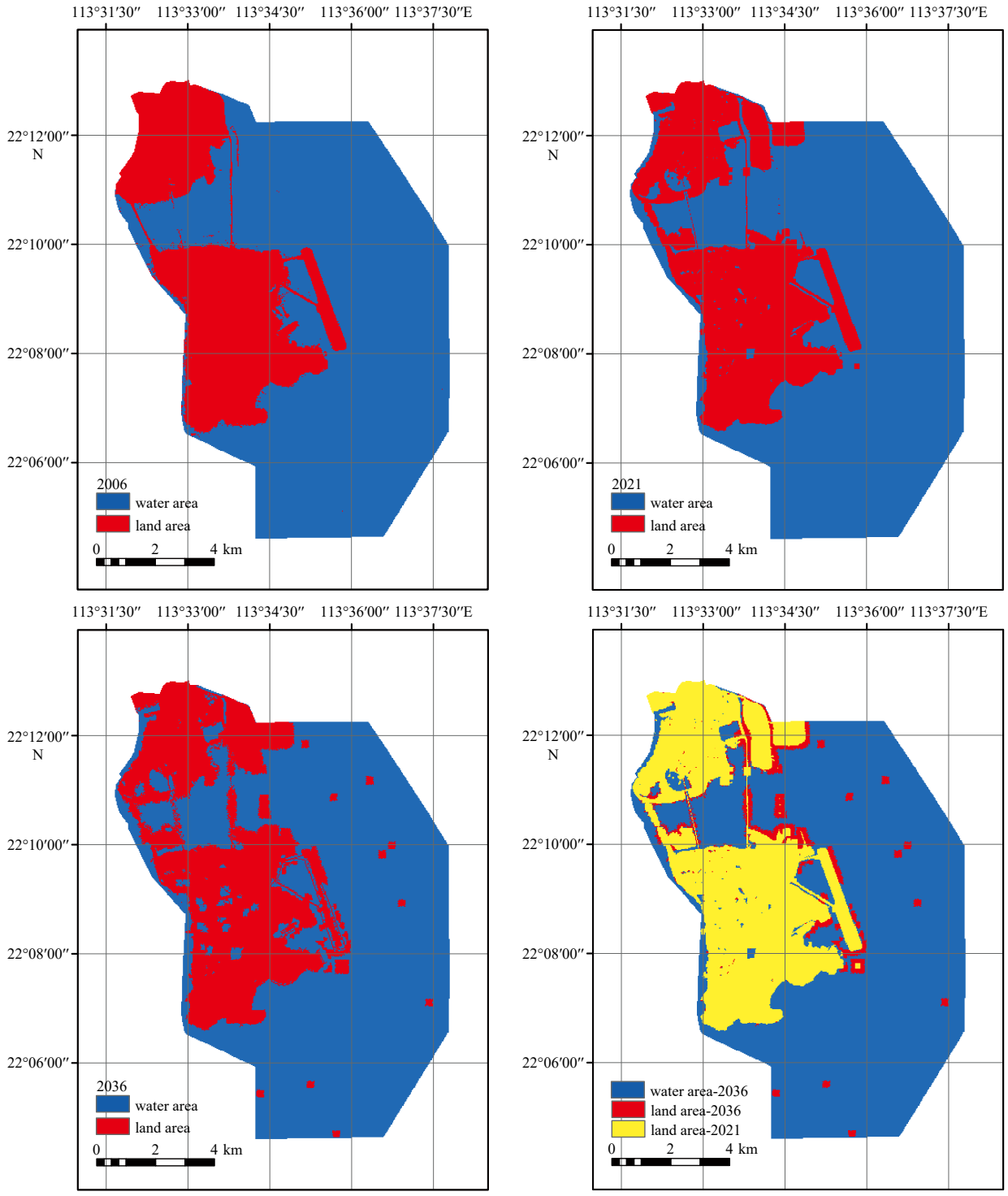


**Fig. 9.** Prediction of the water body range in 2036 and other years based on the PLUS model.

ation has become an important means of expanding the land area of the region, and it is essential to monitor coastline changes. This study uses GEE to calculate the MNDWI water index, extracting the water range of the area combined with Jenks natural discontinuity method and neural net classification, and then the shoreline morphology of the area is statistically analyzed.

This study randomly selected 100 sample points for validation. The verification results indicate that both the overall accuracy and Kappa coefficient of water extraction are high, indicating that the MNDWI, Jenks natural discontinuity method and neural net classification used in this study have a high computational accuracy.

The PLUS model was used to calculate the contribution of different influencing factors to shoreline changes, and the main influencing factors of shoreline changes were analyzed. The study found that social and economic factors such as transportation had a significant impact on shoreline changes, providing extremely valuable references for economic development and land reclamation.

**References**


Adrian J, Sagan V, Maimaitijiang M. 2021. Sentinel SAR-optical fusion for crop type mapping using deep learning and Google Earth Engine. ISPRS Journal of Photogrammetry and Remote Sensing, 175: 215–235, doi: 10.1016/j.isprsjprs.2021.02.018

Ahmad S K, Hossain F, Eldardiry H, et al. 2020. A fusion approach for water area classification using visible, near infrared and synthetic aperture radar for South Asian conditions. IEEE Transactions on Geoscience and Remote Sensing, 58(4): 2471–2480, doi: 10.1109/TGRS.2019.2950705

Andréfouët S, Claereboudt M, Matsakis P, et al. 2001a. Typology of atoll rims in Tuamotu Archipelago (French Polynesia) at landscape scale using SPOT HRV images. International Journal of Remote Sensing, 22(6): 987–1004, doi: 10.1080/01431160 1300074522

Andréfouët S, Kramer P, Torres-Pulliza D, et al. 2003. Multi-site evaluation of IKONOS data for classification of tropical coral reef environments. Remote Sensing of Environment, 88(1–2): 128–143, doi: 10.1016/j.rse.2003.04.005

Andréfouët S, Muller-Karger F E, Hochberg E J, et al. 2001b. Change detection in shallow coral reef environments using Landsat 7 ETM+ data. Remote Sensing of Environment, 78(1–2): 150–162, doi: 10.1016/S0034-4257(01)00256-5

Bendixen M, Lønsmann Iversen L, Anker Bjørk A, et al. 2017. Delta progradation in Greenland driven by increasing glacial mass loss. Nature, 550(7674): 101–104, doi: 10.1038/nature23873

Chen Chao, Chen Huixin, Liang Jintao, et al. 2022. Extraction of water body information from remote sensing imagery while considering greenness and wetness based on Tasseled Cap Transformation. Remote Sensing, 14(3): 3001

Chen Liang-Chieh, Papandreou G, Kokkinos I, et al. 2018. DeepLab: semantic image segmentation with deep convolutional nets, Atrous convolution, and fully connected CRFs. IEEE Transactions on Pattern Analysis and Machine Intelligence, 40(4): 834–848, doi: 10.1109/TPAMI.2017.2699184

Chen Hongruixuan, Wu Chen, Du Bo, et al. 2020. Change detection in multisource VHR images via deep Siamese convolutional multiple-layers recurrent neural network. IEEE Transactions on Geoscience and Remote Sensing, 58(4): 2848–2864, doi: 10.1109/TGRS.2019.2956756

Dai Chunli, Howat I M, Larour E, et al. 2019. Coastline extraction from repeat high resolution satellite imagery. Remote Sensing of Environment, 229: 260–270, doi: 10.1016/j.rse.2019.04.010

Duan Lunhao, Hu Xiangyun. 2020. Multiscale refinement network for water-body segmentation in high-resolution satellite imagery. IEEE Geoscience and Remote Sensing Letters, 17(4): 686–690, doi: 10.1109/LGRS.2019.2926412

Feng Quanlong, Chen Bo'an, Li Guoqing, et al. 2022b. A review for sample datasets of remote sensing imagery. National Remote Sensing Bulletin (in Chinese), 26(4): 589–605, doi: 10.11834/jrs.20221162

Feng Quanlong, Niu Bowen, Zhu Dehai, et al. 2022a. Review for deep learning in land use and land cover remote sensing classification. Transactions of the Chinese Society of Agricultural Machinery (in Chinese), 53(3): 1–17

Feng Wenqing, Sui Haigang, Huang Weiming, et al. 2019. Water body extraction from very high-resolution remote sensing imagery using Deep U-Net and a Superpixel-Based Conditional Random Field Model. IEEE Geoscience and Remote Sensing Letters, 16(4): 618–622, doi: 10.1109/LGRS.2018.2879492

Feyisa G L, Meilby H, Fensholt R, et al. 2014. Automated Water Extraction Index: A new technique for surface water mapping using Landsat imagery. Remote Sensing of Environment, 140: 23–35, doi: 10.1016/j.rse.2013.08.029

Gao Feng, Wang Xiao, Gao Yunhao, et al. 2019. Sea ice change detection in SAR images based on convolutional-wavelet neural networks. IEEE Geoscience and Remote Sensing Letters, 16(8): 1240–1244, doi: 10.1109/LGRS.2019.2895656

Garajeh M K, Malakyar F, Weng Qihao, et al. 2021. An automated deep learning convolutional neural network algorithm applied for soil salinity distribution mapping in Lake Urmia, Iran. Science of the Total Environment, 778: 146253, doi: 10.1016/j.scitotenv.2021.146253

Ge Chuangjie, Xie Wenjun, Meng Lingkui. 2022. Extracting lakes and reservoirs from GF-1 satellite imagery over China using improved U-Net. IEEE Geoscience and Remote Sensing Letters, 19: 1504105

Geusebroek J M, Smeulders A W M, van de Weijer J. 2003. Fast anisotropic Gauss filtering. IEEE Transactions on Image Processing, 12(8): 938–943, doi: 10.1109/TIP.2003.812429

Gong Maoguo, Zhou Zhiqiang, Ma Jingjing. 2012. Change detection in synthetic aperture radar images based on image fusion and fuzzy clustering. IEEE Transactions on Image Processing, 21(4): 2141–2151, doi: 10.1109/TIP.2011.2170702

Hertel V, Chow C, Wani O, et al. 2023. Probabilistic SAR-based water segmentation with adapted Bayesian convolutional neural network. Remote Sensing of Environment, 285: 113388, doi: 10.1016/j.rse.2022.113388

Hinton G E, Salakhutdinov R R. 2006. Reducing the dimensionality of data with neural networks. Science, 313(5786): 504–507, doi: 10.1126/science.1127647

Hochberg E. 2003. Spectral reflectance of coral reef bottom-types worldwide and implications for coral reef remote sensing. Remote Sensing of Environment, 85(2): 159–173, doi: 10.1016/S0034-4257(02)00201-8

Houborg R, McCabe M F. 2018. Daily retrieval of NDVI and LAI at 3 m resolution via the fusion of CubeSat, Landsat, and MODIS data. Remote Sensing, 10(6): 890, doi: 10.3390/rs10060890

Hu Hongtao, Ban Yifang. 2014. Unsupervised change detection in multitemporal SAR images over large urban areas. IEEE Journal of Selected Topics in Applied Earth Observations and Remote Sensing, 7(8): 3248–3261, doi: 10.1109/JSTARS.2014.2344017

Islam M M, Borgqvist H, Kumar L. 2019. Monitoring mangrove forest landcover changes in the coastline of Bangladesh from 1976 to 2015. Geocarto International, 34(13): 1458–1476, doi: 10.1080/10106049.2018.1489423

Jiang Wei, He Guojin, Long Tengfei, et al. 2018. Multilayer perceptron neural network for surface water extraction in Landsat 8 OLI satellite images. Remote Sensing, 10(5): 755, doi: 10.3390/rs10050755

Karaman M. 2021. Comparison of thresholding methods for shoreline extraction from Sentinel-2 and Landsat-8 imagery: Extreme Lake Salda, track of Mars on Earth. Journal of Environmental Management, 298: 113481, doi: 10.1016/j.jenvman.2021.113481

Li A S, Chirayath V, Segal-Rozenhaimer M, et al. 2020. NASA NeMO-Net's convolutional neural network: mapping marine habitats with spectrally heterogeneous remote sensing imagery. IEEE Journal of Selected Topics in Applied Earth Observations and Remote Sensing, 13: 5115–5133, doi: 10.1109/JSTARS.2020.3018719

Li Xiang, Fu Jingying, Jiang Dong, et al. 2022a. Land use optimization in Ningbo City with a coupled GA and PLUS model. Journal of Cleaner Production, 375: 134004, doi: 10.1016/j.jclepro.2022.134004

Li Ruirui, Liu Wenjie, Yang Lei, et al. 2018. DeepUNet: A deep fully convolutional network for pixel-level Sea-Land segmentation. IEEE Journal of Selected Topics in Applied Earth Observations and Remote Sensing, 11(11): 3954–3962, doi: 10.1109/JSTARS.2018.2833382

Li Junjie, Meng Yizhuo, Li Yuanxi, et al. 2022b. Accurate water extraction using remote sensing imagery based on normalized difference water index and unsupervised deep learning. Journal of Hydrology, 612: 128202, doi: 10.1016/j.jhydrol.2022.128202

Li Yangyang, Peng Cheng, Chen Yanqiao, et al. 2019. A deep learning method for change detection in synthetic aperture radar images. IEEE Transactions on Geoscience and Remote Sensing, 57(8): 5751–5763, doi: 10.1109/TGRS.2019.2901945

Liu Xulong, Deng Ruru, Xu Jianhui, et al. 2017. Spatiotemporal evolution characteristics of coastlines and driving force analysis of the Zhujiang River Estuary in the past 40 years. Journal of Geo-

information Science, 19(10): 1336–1345
Lu Ming, Fang Leyuan, Li Muxing, et al. 2022. NFANet: A novel method for weakly supervised water extraction from high-resolution remote-sensing imagery. IEEE Transactions on Geoscience and Remote Sensing, 60: 5617114
Lunetta R S, Knight J F, Ediriwickrema J, et al. 2006. Land-cover change detection using multi-temporal MODIS NDVI data. Remote Sensing of Environment, 105(2): 142–154, doi: 10.1016/j.rse.2006.06.018
McCarthy G D, Haigh I D, Hirschi J J M, et al. 2015. Ocean impact on decadal Atlantic climate variability revealed by sea-level observations. Nature, 521(7553): 508–510, doi: 10.1038/nature14491
Mcfeeters S K. 1996. The use of the Normalized Difference Water Index (NDWI) in the delineation of open water features. International Journal of Remote Sensing, 17(7): 1425–1432, doi: 10.1080/01431169608948714
Mumby P J, Edwards A J. 2002. Mapping marine environments with IKONOS imagery: enhanced spatial resolution can deliver greater thematic accuracy. Remote Sensing of Environment, 82(2–3): 248–257, doi: 10.1016/S0034-4257(02)00041-X
Nemni E, Bullock J, Belabbes S, et al. 2020. Fully convolutional neural network for rapid flood segmentation in synthetic aperture radar imagery. Remote Sensing, 12(16): 2532, doi: 10.3390/rs12162532
Ni Jun, Zhang Fan, Yin Qiang, et al. 2021. Random neighbor pixel-block-based deep recurrent learning for polarimetric SAR image classification. IEEE Transactions on Geoscience and Remote Sensing, 59(9): 7557–7569, doi: 10.1109/TGRS.2020.3037209
Pham B T, Bui D T, Prakash I, et al. 2017. Hybrid integration of Multilayer Perceptron Neural Networks and machine learning ensembles for landslide susceptibility assessment at Himalayan area (India) using GIS. CATENA, 149: 52–63, doi: 10.1016/j.catena.2016.09.007
Purkis S, Kenter J A M, Oikonomou E K, et al. 2002. High-resolution ground verification, cluster analysis and optical model of reef substrate coverage on Landsat TM imagery (Red Sea, Egypt). International Journal of Remote Sensing, 23(8): 1677–1698, doi: 10.1080/01431160110047722
Qiu Chunping, Mou Lichao, Schmitt M, et al. 2020. Fusing multiseasonal Sentinel-2 imagery for urban land cover classification with multibranch residual convolutional neural networks. IEEE Geoscience and Remote Sensing Letters, 17(10): 1787–1791, doi: 10.1109/LGRS.2019.2953497
Rokni K, Ahmad A, Selamat A, et al. 2014. Water feature extraction and change detection using multitemporal landsat imagery. Remote Sensing, 6(5): 4173–4189, doi: 10.3390/rs6054173
Saxena N, Rathore N. 2013. A review on speckle noise filtering techniques for SAR images. International Journal of Advanced Research in Computer Science and Electronics Engineering, 2(2): 243–247
Seo D K, Yong H K, Yang D E, et al. 2018. Fusion of SAR and multispectral images using random forest regression for change detection. ISPRS International Journal of Geo-Information, 7(10): 401, doi: 10.3390/ijgi7100401
Sunder S, Ramsankaran R, Ramakrishnan B. 2017. Erratum to: Intercomparison of remote sensing-based shoreline mapping techniques at different coastal stretches of India. Environmental Monitoring and Assessment, 189(7): 334, doi: 10.1007/s10661-017-6046-8
Tseng S H, Sun Weihao. 2022. Sea–land segmentation using HED-UNET for monitoring Kaohsiung Port. Mathematics, 10(22): 4202, doi: 10.3390/math10224202
Wang Guoli, Fan Bin, Xiang Shiming, et al. 2017. Aggregating rich hierarchical features for scene classification in remote sensing imagery. IEEE Journal of Selected Topics in Applied Earth Observations and Remote Sensing, 10(9): 4104–4115, doi: 10.1109/JSTARS.2017.2705419
Wang Lijuan, Niu Zheng, Zhao Degang, et al. 2010. The study of coastline extraction and validation using ETM remote sensing image. Remote Sensing Technology and Application, 25(2): 235–239
Wang Jin, Wu Zhifeng, Li Shaoying, et al. 2016. Coastline and land use change detection and analysis with remote sensing in the Zhujiang River Estuary Gulf. Scientia Geographica Sinica (in Chinese), 36(12): 1903–1911
Wang Xiaobiao, Xie Shunping, Zhang Xueliang, et al. 2018a. A robust Multi-Band Water Index (MBWI) for automated extraction of surface water from Landsat 8 OLI imagery. International Journal of Applied Earth Observation and Geoinformation, 68: 73–91, doi: 10.1016/j.jag.2018.01.018
Wang Li, Wang Huan. 2019. Water hazard detection using conditional generative adversarial network with mixture reflection attention units. IEEE Access, 7: 167497–167506, doi: 10.1109/ACCESS.2019.2953768
Wang Xiaoping, Zhang Fei, Ding Jianli, et al. 2018b. Estimation of soil salt content (SSC) in the Ebinur Lake Wetland National Nature Reserve (ELWNNR), Northwest China, based on a Bootstrap-BP neural network model and optimal spectral indices. Science of the Total Environment, 615: 918–930, doi: 10.1016/j.scitotenv.2017.10.025
Wei Jiawei, Feng Lian, Tong Yan, et al. 2023. Long-term observation of global nuclear power plants thermal plumes using Landsat images and deep learning. Remote Sensing of Environment, 295: 113707, doi: 10.1016/j.rse.2023.113707
Wei Qinyu, Nurmemet I, Gao Minhua, et al. 2022. Inversion of soil salinity using multisource remote sensing data and particle swarm machine learning models in Keriya Oasis, Northwestern China. Remote Sensing, 14(3): 512, doi: 10.3390/rs14030512
Weng Liguo, Xu Yiming, Xia Min, et al. 2020. Water areas segmentation from remote sensing images using a separable residual SegNet network. ISPRS International Journal of Geo-Information, 9(4): 256, doi: 10.3390/ijgi9040256
Wieland M, Martinis S, Kiefl R, et al. 2023. Semantic segmentation of water bodies in very high-resolution satellite and aerial images. Remote Sensing of Environment, 287: 113452, doi: 10.1016/j.rse.2023.113452
Xie Huarong, Xu Qing, Zheng Quanan, et al. 2022. Assessment of theoretical approaches to derivation of internal solitary wave parameters from multi-satellite images near the Dongsha Atoll of the South China Sea. Acta Oceanologica Sinica, 41(6): 137–145, doi: 10.1007/s13131-022-2015-3
Xu Hanqiu. 2005. A study on information extraction of water body with the modified normalized difference water index (MNDWI). Journal of Remote Sensing (in Chinese), 9(5): 589–595
Xue Weibao, Yang Hui, Wu Yanlan, et al. 2021. Water body automated extraction in polarization SAR images with dense-coordinate-feature-concatenate network. IEEE Journal of Selected Topics in Applied Earth Observations and Remote Sensing, 14: 12073–12087, doi: 10.1109/JSTARS.2021.3129182
Yang Chenchen, Gan Huayang, Wan Rongsheng, et al. 2021. Spatiotemporal evolution and influencing factors of coastline in the Guangdong-Hong Kong-Macao Greater Bay Area from 1975 to 2018. Geology in China (in Chinese), 48(3): 697–707
Yang Xiucheng, Qin Qiming, Grussenmeyer P, et al. 2018. Urban surface water body detection with suppressed built-up noise based on water indices from Sentinel-2 MSI imagery. Remote Sensing of Environment, 219: 259–270, doi: 10.1016/j.rse.2018.09.016
Yang Jiechao, Wang Xuelei, Wang Ruihua, et al. 2020. Combination of convolutional neural networks and recurrent neural networks for predicting soil properties using VIS–NIR spectroscopy. Geoderma, 380: 114616, doi: 10.1016/j.geoderma.2020.114616
Yao Fangfang, Wang Jida, Wang Chao, et al. 2019. Constructing long-term high-frequency time series of global lake and reservoir areas using Landsat imagery. Remote Sensing of Environment, 232: 111210, doi: 10.1016/j.rse.2019.111210
Yousif O, Ban Yifang. 2014. Improving SAR-based urban change detection by combining MAP-MRF classifier and nonlocal means similarity weights. IEEE Journal of Selected Topics in Applied Earth Observations and Remote Sensing, 7(10): 4288–4300, doi:

10.1109/JSTARS.2014.2347171

Zhang Fan, Du Bo, Zhang Liangpei. 2016. Scene classification via a gradient boosting random convolutional network framework. IEEE Transactions on Geoscience and Remote Sensing, 54(3): 1793–1802, doi: 10.1109/TGRS.2015.2488681

Zhang Qianqian, Li Li, Sun Ruizhi, et al. 2022b. Retrieval of the soil salinity from Sentinel-1 Dual-Polarized SAR data based on deep neural network regression. IEEE Geoscience and Remote Sensing Letters, 19: 4006905

Zhang Zhengxin, Liu Qingjie, Wang Yunhong. 2018. Road extraction by deep residual U-Net. IEEE Geoscience and Remote Sensing Letters, 15(5): 749–753, doi: 10.1109/LGRS.2018.2802944

Zhang Tianyuan, Ren Huazhong, Qin Qiming, et al. 2017b. Surface water extraction from Landsat 8 OLI imagery using the LBV transformation. IEEE Journal of Selected Topics in Applied Earth Observations and Remote Sensing, 10(10): 4417–4429, doi: 10.1109/JSTARS.2017.2719029

Zhang Guanjin, Roslan S N A B, Wang Ci, et al. 2023. Research on land cover classification of multi-source remote sensing data based on improved U-net network. Scientific Reports, 13(1): 16275, doi: 10.1038/s41598-023-43317-1

Zhang Zhimian, Wang Haipeng, Xu Feng, et al. 2017a. Complex-valued convolutional neural network and its application in polarimetric SAR image classification. IEEE Transactions on Geoscience and Remote Sensing, 55(12): 7177–7188, doi: 10.1109/TGRS.2017.2743222

Zhang Jinsong, Xing Mengdao, Sun Guangcai, et al. 2021. Water body detection in high-resolution SAR images with cascaded fully-convolutional network and variable focal loss. IEEE Transactions on Geoscience and Remote Sensing, 59(1): 316–332, doi: 10.1109/TGRS.2020.2999405

Zhang Lin, Yuan Feiniu, Zhang Wenrui, et al. 2020. Review of fully convolutional neural network. Computer Engineering and Applications (in Chinese), 56(1): 25–37

Zhang Shihe, Zhong Quanlin, Cheng Dongliang, et al. 2022a. Landscape ecological risk projection based on the PLUS model under the localized shared socioeconomic pathways in the Fujian Delta region. Ecological Indicators, 136: 108642, doi: 10.1016/j.ecolind.2022.108642

Zhao Wenzhi, Du Shihong. 2016. Learning multiscale and deep representations for classifying remotely sensed imagery. ISPRS Journal of Photogrammetry and Remote Sensing, 113: 155–165, doi: 10.1016/j.isprsjprs.2016.01.004